Title	H2 generation and sulfide to sulfoxide oxidation in H2O using sunlight with a model photoelectrosynthesis cell
Author(s)	Farràs, Pau; Di Giovanni, Carlo; Clifford, John Noel; Palomares, Emilio; Llobet, Antoni
Publication Date	2014-10-28
Publication Information	Farràs, Pau, Di Giovanni, Carlo, Clifford, John Noel, Palomares, Emilio, & Llobet, Antoni. (2015). H2 generation and sulfide to sulfoxide oxidation with H2O and sunlight with a model photoelectrosynthesis cell. Coordination Chemistry Reviews, 304–305, 202-208. doi: http://dx.doi.org/10.1016/j.ccr.2014.10.007
Publisher	Elsevier
Link to publisher's version	http:/dx.doi.org/10.1016/j.ccr.2014.10.007
Item record	http://hdl.handle.net/10379/5956
DOI	http://dx.doi.org/10.1016/j.ccr.2014.10.007

H_2 Generation and Sulfide to Sulfoxide Oxidation with H_2O and Sunlight with a Model Photoelectrosynthesis Cell

Pau Farràs,[a] Carlo Di Giovanni,[a] John Noel Clifford,[a] Emilio Palomares[*,a,b] and Antoni Llobet[*,a,c]

[a] Institute of Chemical Research of Catalonia (ICIQ), Avinguda Països Catalans 16, E-43007 Tarragona, Spain.

[b] ICREA, Avda. Lluís Companys 28, Barcelona E-08030, Spain.

[c] Departament de Química, Universitat Autònoma de Barcelona, Cerdanyola del Vallès, 08193 Barcelona, Spain.

Corresponding Authors

* E-mail: allobet@iciq.cat. (A. L.)

* E-mail: epalomares@iciq.cat. (E. P.)

ABSTRACT

A summary of the recent advances in homogeneous light-driven catalytic oxidation reactions is provided either using sacrificial agents or with complete functional cells. In this work, a photoelectrosynthesis model cell (PESC) for H_2 generation together with methyl phenyl sulfide (MeSPh) oxidation to the corresponding sulfoxide (MeSPh) with H_2O and using sunlight has been prepared and characterized. We have built a two compartment PESC connected through a Nafion proton exchange membrane. The cathode consists of a platinum mesh in a pH 7.0 buffered solution. The photoanode consist on a FTO/TiO_2-P-bpy-$Ru^{II,2+}$ (where P-bpy-$Ru^{II,2+}$ is $[Ru^{II}(P\text{-}bpy)(bpy)_2]^{2+}$ and P-bpy is 2,2'-bipyridine-4,4'-bis(phosphonic acid)) electrode immersed in the same pH 7.0 solution. The anodic compartment also contains the catalyst $\{[Ru^{II}(trpy)(H_2O)]_2(\mu\text{-}pyr\text{-}dc)\}(OAc)$ (trpy is 2,2':6',2"-terpyridine and pyr-dc^{3-} is the pyrazolato-3,5-dicarboxylato trianion) abbreviated as $[H_2O\text{-}Ru^{II}Ru^{II}\text{-}OH_2]^{+}$ (**2**,**2**$^{+}$) in homogenous solution. The illumination under sun simulated 1.5 AMG (100 mW cm^{-2}) together with an external input of -0.43 V *vs.* SSCE led to the formation of hydrogen gas and the oxidation of the sulfide to sulfoxide. Last but not least, all the significant reactions involved have been characterized both from a thermodynamic and also from a kinetics viewpoint to analyze the system losses.

KEYWORDS: Photoelectrosynthesis, Photochemistry, Photoanodes, Redox Catalysis, Ruthenium Complexes, Sulfide Oxidation.

Research highlights

- Proof of concept PESC cell for oxidation of sulfides and hydrogen production.
- The use of homogeneous catalysts in PESC cells is demonstrated.
- First example of a complete thermodynamic and kinetic characterization of a photoelectrosynthesis cell.
- A molecular system for light-harvesting and catalytic photooxidation of sulfides is shown.

Graphical Abstract

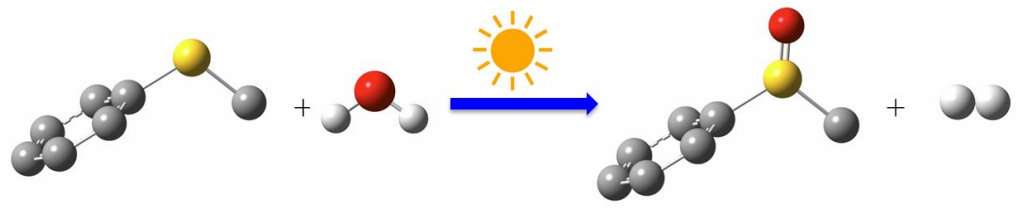

1. Introduction

The area of light-driven oxidation reactions has experienced a large development in recent years due to the renovated interest in the generation of solar fuels. Current and predicted worldwide energy demands are unsustainable with carbon-based fuels and a transition from fossil to solar fuels is urgently needed [1,2,3]. Many different strategies have been adopted by the scientific community to generate solar fuels, from material-based to molecular systems, and even the combination of both. Moreover, a solar fuel such as hydrogen can be potentially produced either by the oxidation of water (best case scenario), or by the oxidation of an organic substrate with water. Only until recently, most of the light-driven oxidation systems used sacrificial reagents to avoid unwanted recombination reactions. This review will only focus on molecular systems and will provide the reader with an example of a functional photoelectrosynthesis cell for the oxidation of an organic substrate and the generation of H_2.

2. Sacrificial molecular systems

2.1 Light-driven water oxidation

The discovery in the mid-80s of molecular catalysts for water oxidation led to the first examples of 3-component systems for light-driven oxidation of water. They comprised of a molecular ruthenium catalyst, a photosensitizer and a sacrificial electron acceptor. However, their stability and performance was very limited [4,5]. In both cases $[Ru(bpy)_3]^{2+}$ and $Na_2S_2O_8$ were used as photosensitizer and sacrificial electron acceptor, respectively. After 20 years, the synthesis of more efficient water oxidation catalysts with lower overpotentials has fostered the generation of

more 3-component systems with better efficiencies. Molecular catalysts based on mononuclear and dinuclear Ru-complexes [6,7,8,9,10], Ru polyoxometallates (Ru-POM) [11] and iron complexes [12] have shown activity under sacrificial conditions. Some of them have demonstrated good activities towards water oxidation when using $[Co(NH_3)_5Cl]Cl_2$ [7,8] as sacrificial acceptor.

More sophisticated molecular systems have been prepared by combining catalytic and light-harvesting units on the same molecules. These dyad systems are Ru-based photocatalysts that are able to oxidize water in a 2-component system with a sacrificial reagent. Although their catalytic activity is low, it represents a breakthrough in the area by opening new possibilities as photocatalysts for water oxidation. In all examples described, the activity of the dyad is higher than the two separate components, a phenomenon ascribed to fast intramolecular electron transfer kinetics that allows to reach the needed active higher oxidation states of the catalyst [13,14]. However, all the examples above are based on sacrificial reagents and the products generated, shown in equation 1, are oxygen and protons. The latter need to be reduced elsewhere to produce the desired solar fuel.

$$2\,H_2O \xrightarrow{4\,h\nu} O_2 + 4H^+ + 4e^- \qquad E^0 = 1.23\ V \qquad (1)$$

2.2 Light-driven oxidation of organic substrates

The oxidation of organic substrates with water and sunlight is a challenge that has important implications both for basic research science and for the green chemical industry. A model

example of this is the oxidation of sulfides to sulfoxides as indicated in the equation below for the particular case of methyl phenyl sulfide (MeSPh) [15],

$$\mathrm{MeSPh} + \mathrm{H_2O} \xrightarrow{2\ h\nu} \mathrm{MeS(O)Ph} + \mathrm{H_2} \quad \Delta G^{o} \cong 31.6\ \mathrm{kcal/mol} \qquad (2)$$

As drawn, this reaction takes place in 100% atom economy and it generates a sulfoxide, which is a highly added value product, using water and sunlight. Moreover, using sunlight and water avoids the use of expensive and not very environmentally friendly oxidants such as CrO_3 or MnO_4^-. Furthermore, it generates molecular hydrogen that is a green carbon-free fuel vector [16].

One approach of achieving this overall reaction is via a photoelectrochemical cell (PEC). The overall reaction in equation 2 can be divided in two half reactions occurring at the anode and cathode as indicated below,

$$\text{Anode:} \quad \mathrm{MeSPh} + \mathrm{H_2O} \longrightarrow \mathrm{MeS(O)Ph} + 2\mathrm{H^+} + 2\mathrm{e^-} \qquad (3)$$

$$\text{Cathode:} \quad 2\mathrm{H^+} + 2\mathrm{e^-} \longrightarrow \mathrm{H_2} \qquad (4)$$

The overall reaction 2, is thermodynamically not favored and thus the need of an external energy input such as light to drive it. Since sunlight interacts with H_2O and MeSPh mainly at a vibrational level a series of additional reactions involving light harvesting molecules needs to be designed and coupled to suitable catalysts in order to break and form the desired bonds at a reasonable rate.

The oxidation of substrates with visible light as indicated in the anodic equation 3, has been described in the literature using $[Ru(bpy)_3]^{2+}$ (bpy is 2,2'-bypyridine) as a light harvesting molecule coupled to a sacrificial electron acceptor (SEA), such as sodium persulfate or Co(III) salts like $[Co(NH_3)_5Cl]^{2+}$ [17,18]. As before, dyad systems with catalytic and photosensitizer units in the same molecule have shown good turnover numbers (TN) for the oxidation of a large variety of substrates, such as alcohols, sulfides and alkenes [19,20,21,22,23,24,25,26].

The oxidation of sulfide to sulfoxide involves formally the addition of an oxygen atom to the sulfur atom. Thus, ideal catalysts for this transformation will involve typical transition metal complexes in high oxidation states containing the M=O group. Ru(II)-aqua polypyridyl complexes in general have been described to carry out PCET type of reactions, reaching highly reactive Ru(IV)=O species [27]. The latter is an excellent O-atom transfer oxidant with regard to the oxidation of alkenes to epoxides and sulfides to sulfoxides [28]. For this reason we have chosen the dinuclear Ru-aqua complex, $\{[Ru^{II}(trpy)(H_2O)]_2(\mu\text{-pyr-dc})\}(OAc)$ (trpy is 2,2':6',2"-terpyridine and pyr-dc^{3-} is the pyrazolato-3,5-dicarboxylato trianion) abbreviated as $[H_2O\text{-}Ru^{II}Ru^{II}\text{-}OH_2]^+$ **(2,2$^+$)**, where the trpy and bridging ligand are not written and whose structure is shown in Chart 1. This complex undergoes a series of PCET processes until it generates the reactive species that is formally in oxidation state IV,IV, $[O\text{-}Ru^{IV}Ru^{IV}\text{-}O]^+$ **(4,4$^+$)**. This catalytic **4,4$^+$** species is highly reactive and can transform alkenes into epoxides (equation 5) [29],

$$[O\text{-}Ru^{IV}Ru^{IV}\text{-}O]^+ + PhCH{=}CHMe + H_2O \rightarrow [HO\text{-}Ru^{III}Ru^{III}\text{-}OH]^+ + PhCH(O)CHMe \quad (5)$$

4,4$^+$ **3,3$^+$**

and organic sulfides to sulfoxides as will be described here (equation 6)**.**

2.2.1. Homogeneous chemical, electrochemical and photochemical catalytic oxidation of MeSPh to MeS(O)Ph. We tested the capacity of **4,4**$^{+}$ to react with sulfides in homogeneous phase, chemically, electrochemically and photochemically.

Electrochemical experiments in aqueous solution at pH 7.0 show that the active catalytic species for sulfide oxidation is the **4,4**$^{+}$ as can be seen in Figure 2, by the presence of an electrocatalytic wave at the foot of the IV,IV oxidation wave ($E^{o}_{IV,IV\text{-}IV,III}$ = 0.74 V). Since the oxidation of sulfide to sulfoxide involves a two electron process the reduced catalytic species, given the two-electron nature of the sulfide oxidation, is $[HO\text{-}Ru^{III}Ru^{III}\text{-}OH]^{+}$, **3,3**$^{+}$, as indicated in equation 6,

$$[O\text{-}Ru^{IV}Ru^{IV}\text{-}O]^{+} + MeSPh + H_2O \rightarrow [HO\text{-}Ru^{III}Ru^{III}\text{-}OH]^{+} + MeS(O)Ph \quad (6)$$

4,4^{+} **3,3**$^{+}$

Chemically, under homogeneous conditions the active catalyst can be generated with PhIO that acts as a sacrificial oxidant according to,

$$[HO\text{-}Ru^{III}Ru^{III}\text{-}OH]^{+} + PhIO \rightarrow [O\text{-}Ru^{IV}Ru^{IV}\text{-}O]^{+} + PhI + H_2O \quad (7)$$

3,3^{+} **4,4**$^{+}$

Thus a catalytic system can be built using **4,4**$^{+}$ 1.0 mM/MeSPh 2.0 M/PhIO 4.0 M/H_2O 4.0 M in DCM:EtOH (1:1). This gives 1.81 M sulfoxide that represents an outstanding 1810 turnover number (TN) with regard to the initial catalyst in 60 minutes. After this time the conversion of the initial substrate reaches a value of 90.5 % with a remarkable TOF_i of 3300 ks^{-1}.

The sulfide oxidation can also be photochemically induced using $[Ru^{II}(bpy)_3]^{2+}$, (abbreviated as **bpy-Ru$^{II,2+}$**; E^o(III/II) = 1.10 V) and $[Co^{III}(NH_3)_5Cl]^{2+}$ (abbreviated as **Co^{III}**) as a sacrificial electron acceptor (SEA). A deoxygenated solution containing **2,2**$^{+}$ 0.02 mM/MeSPh 20 mM/**bpy-Ru$^{II,2+}$** 0.2 mM/**Co^{III}** 20 mM in a 0.05 M sodium phosphate buffer (pH 7.0) was irradiated by visible light for 30 min. Analysis of the product generation showed the formation of 9 mM sulfoxide that represents 450 turnover numbers (TNs) with regard to the initial catalyst. After this time the conversion of the initial substrate reaches a value of 90% with an impressive initial TOF_i of 250 ks^{-1}.

The generation of the active species was achieved sequentially by the photochemically produced **bpy-Ru$^{III,3+}$** according to,

$$2\,[Ru^{III}(bpy)_3]^{3+} + [HO\text{-}Ru^{III}Ru^{III}\text{-}OH]^{+} \rightarrow 2\,[Ru^{II}(bpy)_3]^{2+} + [O\text{-}Ru^{IV}Ru^{IV}\text{-}O]^{+} + 2H^{+} \quad (8)$$

bpy-Ru$^{III,3+}$ **3,3**$^{+}$ **bpy-Ru$^{II,2+}$** **4,4**$^{+}$

The lower TOF_i with regard to the chemical homogenous system is due to lower concentration of Ru(III) that is generated in the photochemically induced experiment. In the previous case the

PhIO was used in a ratio of 1:4000 Cat:PhIO. Nevertheless the large TN achieved enables the present system to be tried under more restrictive conditions such as in heterogeneous phase.

3. Photoelectrochemical cells for the production of solar fuels

3.1 Light-driven water splitting

An ideal functional device for the generation of hydrogen should avoid the use of sacrificial reagents. Many examples can be found in the literature for the production of hydrogen by using molecular catalyst based on transition metal complexes and sacrificial electron donors. The sacrificial agents react fast and in an irreversible manner so that they favor only the desired reactions. Furthermore, a large excess of sacrificial molecules can be used to favor the desired reaction. So far, only one example can be found in which oxidation and reduction reactions are coupled together in a fully homogeneous molecular system for the oxidation of organic substrates and hydrogen [30].

The best molecular catalysts for water oxidation, described in the previous section with sacrificial reagents, have been incorporated in PEC cells, where oxygen and hydrogen are produced in the anode and cathode, respectively. In all cases, oxygen is produced in photoanodes based on dye-sensitized TiO_2 with a $Ru(bpy)_3$-type of complexes or porphyrins, along with a catalyst embedded in a nafion film or attached to the photosensitzer. On the other hand, the cathode consists on a platinum electrode [31,32,33,34,35,36,37,38,39,40]. In general, the PEC cells have shown small photocurrents, low efficiencies and low stability. Meyer et al. have been able to increase the stability of their chromophore-catalyst assembly on the electrode by the

deposition of a TiO_2 layer by atomic layer deposition (ALD), producing a core-shell structure that also enhance the photocurrent of their system [37]. More recently, photoanodes with chromophore-catalyst dyads have also been studied although only minor details are given on the kinetics of the reaction. Recently several papers on the kinetic studies of Ru-sensitized photoanodes in water have been kinetically characterized [41,42].

3.2 Light-driven oxidation of organic substrates

A few examples exist of photocatalytic oxidation of organic substrates mediated by water using PESCs, although this topic is mainly at its infancy and large developments need to be made before it can be used in a generalized manner. One of the important issues that should be overcome for this type of cells is the absence of sacrificial agents which significantly reduced the driving force toward the productive reactions and for this reason most of the PESCs have been described as a *proof of concept* level [43]. Some other examples can be found where the use of UV-light increases the efficiency of the system and even avoids the use of an external bias to generate hydrogen [44,45]. For a functional device to work, UV-light should be discarded as the share of this high-energy light within the solar spectrum is very small and systems based on visible and NIR light-harvesting molecules need to be used. It is thus crucial for the advancement of this topic, to characterize all the reactions involved in this type of cells both from a thermodynamic and kinetic point of view, in order to be able to achieve technologically relevant devices.

3.2.1 The interaction of the sensitized photoanode with the Ru catalyst.

In this work, we wanted to characterize all kinetic parameters affecting the performance of the cell. Given the excellent behavior in homogenous phase we anchored $[Ru^{II}(P\text{-}bpy)(bpy)_2]^{2+}$ (**P-bpy-Ru$^{II,2+}$**; P-bpy is 2,2'-bipyridine-4,4'-bis(phosphonic acid), see Chart 1) into TiO_2 to generate a photoanode, labeled **FTO/TiO$_2$-P-bpy-Ru$^{II,2+}$** with a dye surface coverage of 4.1 x 10^{-8} mol cm^{-2} [46,47]. This photoanode was stable for days in a mixture of 0.1 M Na_2SO_4/0.83 mM NaH_2PO_4/1.17 mM Na_2HPO_4/0.69 M TFE (2,2,2-trifluoroethanol), and was tested with regard to its capacity to interact in homogeneous phase with our sulfoxidation catalyst **3,3$^+$**, generated under controlled potential electrolysis at E^o_{app} = 0.47 V.

Transient absorption spectroscopy (TAS) was used to measure the electron transfer processes in **FTO/TiO$_2$-P-bpy-Ru$^{II,2+}$** following excitation at 450 nm in the presence and absence of different concentrations of **3,3$^+$** (Figure 3) and MeSPh substrate. The absorbance decay after irradiation was measured at 650 nm which is where **bpy-Ru$^{III,3+}$** has a broad absorption band. In the absence of catalyst the system decays with a half lifetime of about 3.3 ms, which is attributed to the recombination reaction shown in eq. 9 (red arrow 6 in Figure 5), once the electron injects into the TiO_2 conduction band which is known to happen within the picosecond time scale [48].

$$(-)TiO_2\text{-P-bpy-}Ru^{III,3+} \rightarrow TiO_2\text{-P-bpy-}Ru^{II,2+} \qquad t_{1/2} \approx 3.3 \text{ ms} \qquad (9)$$

In the presence of the catalyst **3,3$^+$** the **bpy-Ru$^{III,3+}$** signal decays faster as it is reduced by the catalyst according to equations 10 and 11, in a similar manner as it occurs when a dye is regenerated by a red/ox electrolyte in a dye sensitized solar cell (DSC) [49].

$$(-)TiO_2\text{-P-bpy-}Ru^{III,3+} + [HO\text{-}Ru^{III}Ru^{III}\text{-}OH]^+ \rightarrow$$

$$(-)TiO_2\text{-P-bpy-}Ru^{II,2+} + [O\text{-}Ru^{IV}Ru^{III}\text{-}OH]^+ + H^+ \qquad (10)$$

$$(-)TiO_2\text{-P-bpy-}Ru^{III,3+} + [O\text{-}Ru^{IV}Ru^{III}\text{-}OH]^+ \rightarrow$$

$$(-)TiO_2\text{-P-bpy-}Ru^{II,2+} + [O\text{-}Ru^{IV}Ru^{IV}\text{-}O]^+ + H^+ \qquad (11)$$

As the catalyst concentration is increased from 30 to 220 μM the decay of the **bpy-Ru$^{III,3+}$** signal increases by almost an order of magnitude with a $t_{1/2} \approx 0.18$ ms. A dependence of dye regeneration on red/ox couple concentration has also been observed in DSCs [50].

The notable increase in signal intensity at slower timescales (0.1-1 ms) is attributed to the formation of a new species, which we ascribe to the **4,4**$^+$ state of the catalyst. The decay of the **4,4**$^+$ state is due to the oxidation of MeSPh with the catalyst returning to its **3,3**$^+$ state (blue arrow 5 in Figure 5). Due to the low signal to noise ratio of the kinetic traces we were not able to record the transient spectra of the long-lived species, however, we note that the **4,4**$^+$ state of the catalyst (generated from **2,2**$^+$ at an applied potential of 0.89 V *vs*. SSCE at pH 7.0; see SI) also has an absorption band at 650 nm. Moreover, the $t_{1/2}$ of the decay of the **4,4**$^+$ state (7 ms) is in the order of magnitude found for the heterogeneous MeSPh oxidation reaction described in next section.

3.2.2 Photocatalytic Sulfide Oxidation in Heterogeneous Phase.

As in the previous section, the **FTO/TiO_2-P-bpy-$Ru^{II,2+}$** photoanode in the presence of Co(III) as a sacrificial electron acceptor were used to test its performance in heterogeneous phase. The system: **FTO/TiO_2-P-bpy-$Ru^{II,2+}$** (Γ = 6.4 x 10^{-8} mol cm^{-2})/**$2,2^+$** 0.02 mM/MeSPh 20 mM/Co(III) 20 mM/DMF 13 mM in 0.1 M Na_2SO_4/0.83 mM NaH_2PO_4/1.17 mM Na_2HPO_4/0.69 M TFE buffer solution gives 0.87 mM sulfoxide that represents 44 turnover numbers (TNs) with regard to the initial catalyst in 135 minutes. After this time the conversion of the initial substrate reaches a value of 4.3% with a TOF_i of 13 ks^{-1} (see SI for a product generation as a function of time). Again as in the previous occasion the TOF_i is slightly reduced due to the lower amount of **bpy-$Ru^{II,2+}$** generated in the surface of TiO_2 with regard to the **bpy-$Ru^{II,2+}$** used in homogeneous phase. All the above experiments show the capacity of the system to act as a robust photoanode for the oxidation of sulfide to sulfoxide in the presence of Co(III).

3.2.3 PESC Cell Assembly

Based on the good performance of the catalyst both in homogeneous and in hetergenous sacrificial reactions, we have designed a new photoelectrosynthesis cell (PESC) (Figure 1) where the oxidation catalyst is present in homogeneous phase and thus allowing a fine tuning of redox potentials. The oxidation catalyst has to comply with two indispensable requirements: a) the catalyst has to act efficiently with regard to substrate oxidation and b) the active site of the catalyst needs to be generated very fast by the photoanode. For the latter we are using a $[Ru(bpy)_3]^{2+}$ type of molecule attached at the surface of TiO_2 [18]. This cell configuration benefits from the fact that any catalyst that works in homogeneous phase can be immediately incorporated into the cell. In contrast if the catalyst needs to be anchored on solid devices then

the corresponding homologue adequately functionalized will have to be developed. On the other hand using catalysts in homogeneous phase has the serious drawback that the ratio of anchored-photosensibilizing molecule *vs.* catalyst is generally very low.

In order to generate hydrogen, a small external bias is needed when TiO_2 is used as a photoanode [31,33,51]. As previously reported, despite the fact that the conduction band edge of TiO_2 is more negative than the thermodynamic potential of protons to hydrogen, electrons in trap states below this band are not reducing enough to generate hydrogen, and rapidly recombine according to equation 9. Therefore, an applied potential bias is needed to remove the electrons from the quasi-Fermi level of the semiconductor and transfer them to the cathodic side of a potential PEC. The energy level is dependent on the pH and the applied potential needs to be measured for each system. In our cell using Pt-mesh as a cathode, the potential turned out to be -0.43 V as deduced from the *I-V* curve shown in the SI.

Once the anodic and cathodic sites have been thoroughly studied independently, with the thermodynamics and kinetics known we connected them in the absence of sacrificial agents. We built a two compartment PESC connected through a Nafion proton exchange membrane as shown schematically in Figure 1, with the photoanode and cathode described in the previous sections. Irradiation by visible-light ($\lambda > 400$ nm, 0.1 W cm^{-2}) and at an applied bias of -0.43 V of the three-electrode PESC in 5 mL of 0.1 M Na_2SO_4/0.83 mM NaH_2PO_4/1.17 mM Na_2HPO_4/0.69 M TFE solution, containing **FTO/TiO$_2$-P-bpy-Ru$^{II,2+}$** (Γ = 6.4 x 10^{-8} mol cm^{-2})/**2,2$^+$** 0.09 mM/MeSPh 35 mM/DMF 10 mM produces a photocurrent that decays to a steady 14 μA after 2000 s. In the cathodic compartment 310 nmol of H_2 are formed and a total of 0.067 C

are measured (Figure 4) that corresponds to a faradaic efficiency of 89%. A larger amount of MeS(O)Ph (0.2 mM) could be detected in the anodic compartment by ^{1}H-NMR spectroscopy at the end of the reaction, although its quantitative measurement is associated with a large error. In the absence of the organic substrate or Ru-catalyst or Ru-photosensitizer, the currents obtained as well as product formation were negligible in all cases.

The combination of reactions shown here is a proof of concept of the viability of potential PESCs based on molecular catalysts in homogeneous phase and proper dyes anchored in TiO_2 as photoanodes. However there are a number of unproductive reactions that need to be minimized in order to come up with more efficient cells. These include recombination reactions such as,

$$(-)TiO_2\text{-P-bpy-}Ru^{III,3+} + [HO\text{-}Ru^{III}Ru^{IV}\text{-}O]^{+} + H^{+} \rightarrow TiO_2\text{-P-bpy-}Ru^{III,3+} + [HO\text{-}Ru^{III}Ru^{III}\text{-}OH]^{+} \quad (11)$$

$$(-)TiO_2\text{-P-bpy-}Ru^{III,3+} + [O\text{-}Ru^{IV}Ru^{IV}\text{-}O]^{+} + H^{+} \rightarrow TiO_2\text{-P-bpy-}Ru^{III,3+} + [O\text{-}Ru^{IV}Ru^{III}\text{-}OH]^{+} \quad (12)$$

that are represented as red arrows (7 and 8) in Figure 5.

An additional problem to the cell reported here is the stability of the anchored **P-bpy-Ru$^{II,2+}$** under illumination as the reactions proceed. It can be visually appreciated that the latter slowly deanchors from TiO_2.

4. Conclusions

This review is intended to give a short overview of the light induced oxidative reactions and to show the different steps needed for development of a PESC cell: from the identification of an active oxidation catalyst to its inclusion in a full functional cell for the production of hydrogen. The following is a list of conclusions that can be extracted from the work just presented, together with a graph (Figure 5) that helps to identify all the significant reactions involved in the photoanode.

a) The use of **P-bpy-Ru$^{II,2+}$** sensitizer anchored in TiO_2 facilitates the formation of oxidative species of the catalyst Ru(IV)-Ru(IV) that are active towards the sulfoxidation of MeSPh. Importantly, the III/II redox potential (1.10 V *vs.* SSCE) of the **P-bpy-Ru$^{II,2+}$** sensitizer, is a pre-requisite to be able to generate the sufficient thermodynamic driving force so that the catalyst can reach its active site: the Ru(IV)-Ru(IV) oxidation sate. A lower oxidation potential of the sensitizer will compromise the electron transfer kinetics from the dye to the catalyst and thus no hydrogen or sulfoxide would be generated.

b) The L-TAS shows that the recombination kinetics between the photo-injected electrons at the TiO_2 and the oxidized sensitizer is on the millisecond time scale (reed arrow 6 in Figure 5). Moreover, upon addition of the Ru catalyst the decay becomes bi-phasic with a fast phase corresponding to the efficient regeneration of the oxidized sensitizer (microsecond time scale, arrows 3 and 4, Figure 5) and a second phase that corresponds to the oxidation of the substrate by the high oxidation states of the catalyst (hundreds of miliseconds timescale; arrow 5, Figure 5).

c) The existence of the formation of higher oxidation states derived from $[HO\text{-}Ru^{III}\text{-}Ru^{III}\text{-}OH]^{+}$ is evidenced by the faster decay of Ru^{III} in **FTO/TiO_2-P-bpy-$Ru^{III,3+}$**, in the presence of the catalyst. Furthermore the existence of the two electron oxidized species $[O\text{-}Ru^{IV}\text{-}Ru^{IV}\text{-}O]^{+}$ is indirectly demonstrated by the formation of the sulfoxide, since only the former is capable of carrying out such oxidation.

d) Recombination of the photo-injected electrons at the TiO_2 and the higher oxidation states of the catalyst (red arrows 7-8) are lower than microseconds otherwise these reactions will preclude the formation of the final products.

Finally, we have successfully built, step by step, a complete photoelectrosynthesis cell for simultaneous generation of hydrogen and sulfoxide based on water and sunlight. We have thoroughly studied and characterized all the potential reactions involved both from a thermodynamic and also from a kinetics viewpoint. This work represents a first step towards the use of sunlight and water as sustainable and green oxidation agents using oxidation catalysts in homogeneous pahse, and sets up the basis for the rational development of PESC for pure water splitting with sunlight.

Supporting Information.

Experimental details and additional spectroscopic, electrochemical, and catalytic data.

Acknowledgment

Support by MINECO CTQ-2013-49075-R and “La Caixa” are gratefully acknowledged. CDG is grateful for an FPI grant from MINECO. EP and JC would like to thank ICIQ and ICREA for their financial support.

Chart 1. Schematic drawings of the Ru-photosensitizer $[Ru^{II}(P\text{-}bpy)(bpy)_2]^{2+}$ (**P-bpy-Ru$^{II,2+}$**) and Ru-catalyst ($\{[Ru^{II}(trpy)(H_2O)]_2(\mu\text{-}pyr\text{-}dc)\}^{+}$, **2,2^{+}**, used in this work.

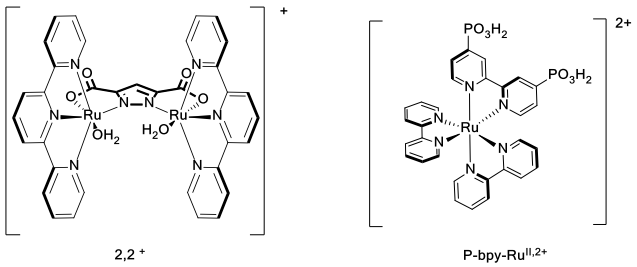

Figure 1. Top, schematic drawing of the two compartment photoelectrochemical cell separated by a proton exchange membrane. Bottom, General Reaction Scheme involving productive reactions. CB: conduction band of TiO_2; D: photosensitizer; D^*: excited state of the photosensitizer; D^+: oxidized photosensitizer; Ru-Cat: sulfoxidation catalyst **2,2**$^+$; PEM: proton exchange membrane, Nafion®.

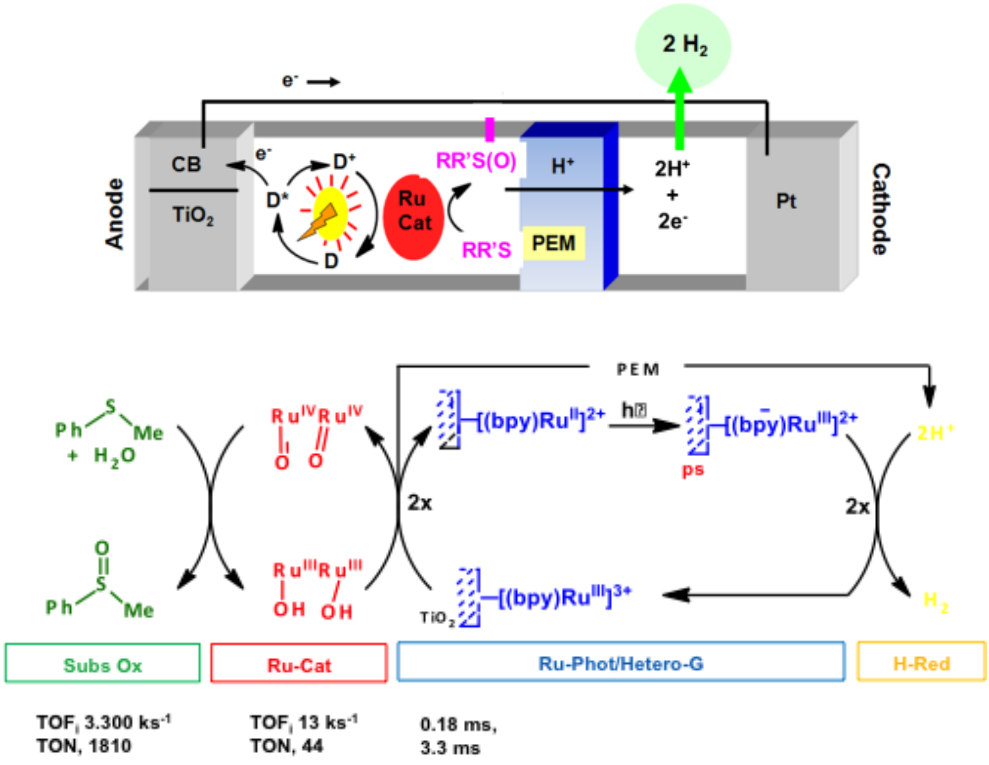

Figure 2. Square-wave voltammogram (SQWV) of **2,2**$^{+}$ in a pH = 7.0 sodium phosphate buffer solution showing the active IV,IV oxidation state (solid line). CV curve of **2,2**$^{+}$ in a pH = 7.0 phosphate buffer in the presence (dashed line) and absence (dotted line) of MeSPh showing the electrocatalytic wave. Starting scan at 0.0 V. A GC disk was used as the working electrode, a platinum wire as the auxiliary electrode, and SSCE as the reference electrode. SQWV parameters: potential increment of 0.004 V, pulse amplitude of 0.025 V, and frequency of 1 Hz.

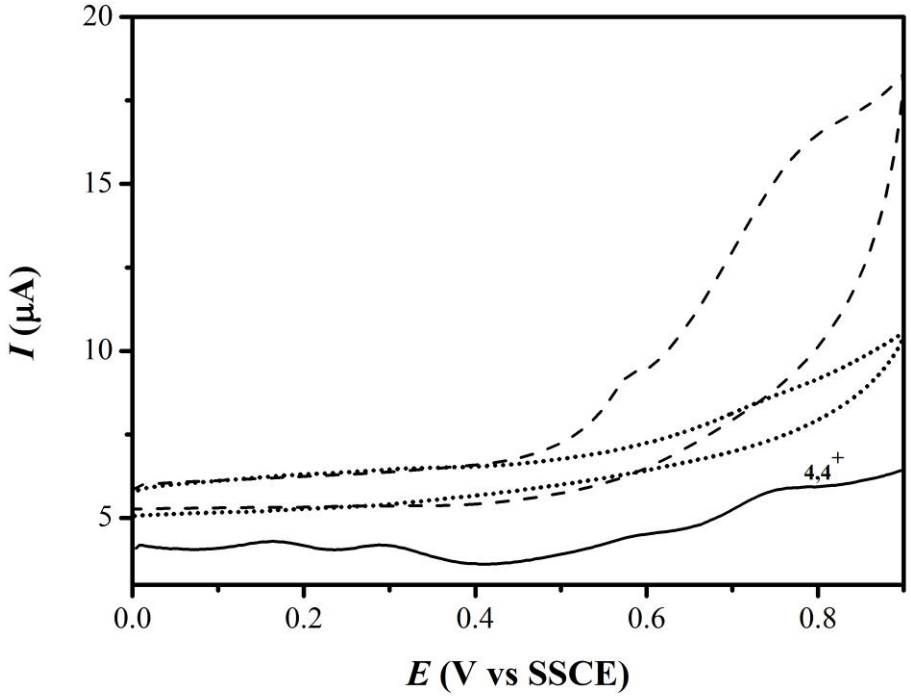

Figure 3. Transient absorption kinetics of **FTO/TiO_2-P-bpy-$Ru^{II,2+}$** photoanodes in a 0.1 M Na_2SO_4/0.83 mM NaH_2PO_4/1.17 mM Na_2HPO_4/0.69 M TFE aqueous solution (blue) in the presence of 42.5 mM MeSPh. Black, in the absence of catalyst; red, with the addition of 30 μM **3,3**$^+$; blue, with the addition of 220 μM **3,3**$^+$. TAS kinetics were recorded under 0.1 Sun illumination (10 mW cm^{-2}) and using laser excitation pulses at 450 nm. TAS kinetics was recorded at 650 nm.

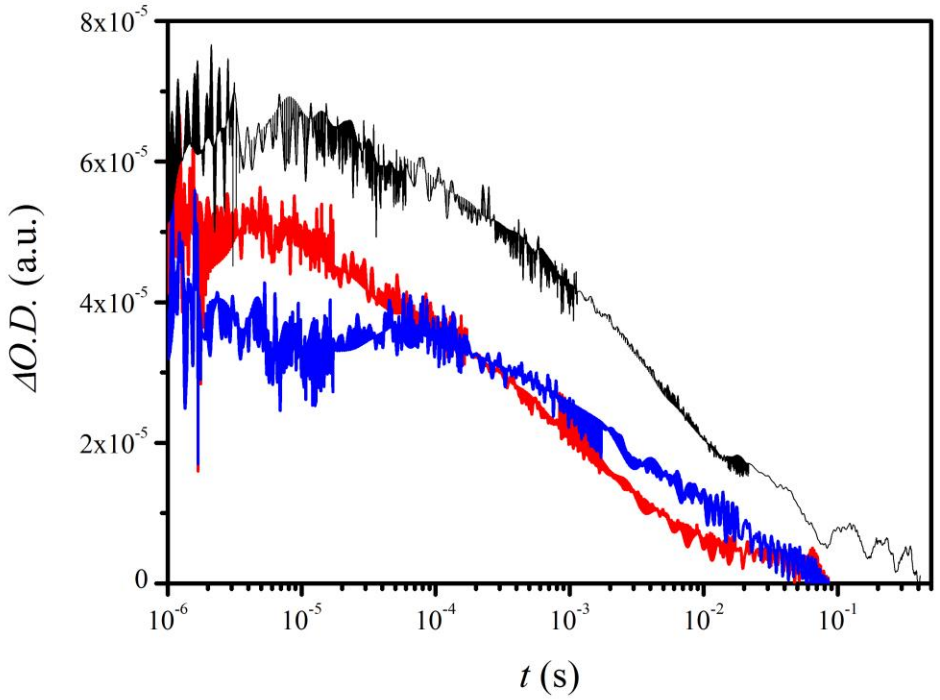

Figure 4. Hydrogen evolution from the cathodic compartment ($V_{gas\ phase}$ = 6.5 mL) measured with a Clark electrode obtained with the PESC cell upon irradiation with a Xe lamp (λ > 400 nm, 0.1 W cm^{-2}) at an applied bias of -0.43 V. The anodic half-cell contains **FTO/TiO_2-P-bpy-$Ru^{II,2+}$** (Γ = 6.4 x 10^{-8} mol cm^{-2})/0.09 mM **$2,2^+$**/MeSPh 35 mM while the cathodic half-cell consists of a Pt mesh. The supporting electrolyte solution is made of a 0.1 M Na_2SO_4/0.83 mM NaH_2PO_4/1.17 mM Na_2HPO_4/0.69 M TFE up to a total volume of 5 mL in each compartment.

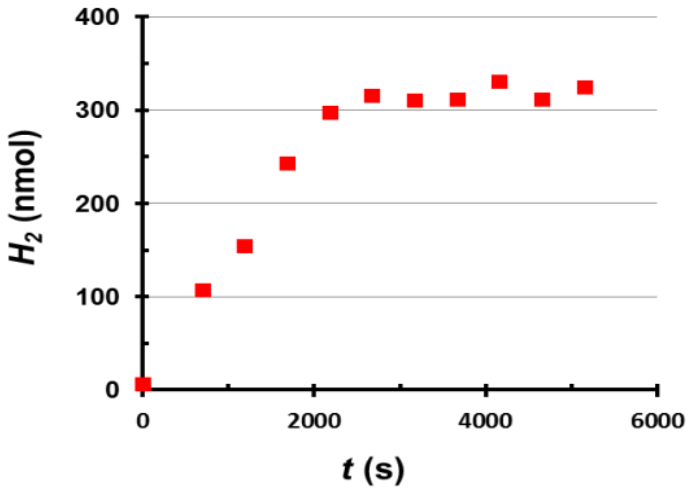

Figure 5. Summary of significant reactions that occur at the anode and their approximate timescales. See text for details.

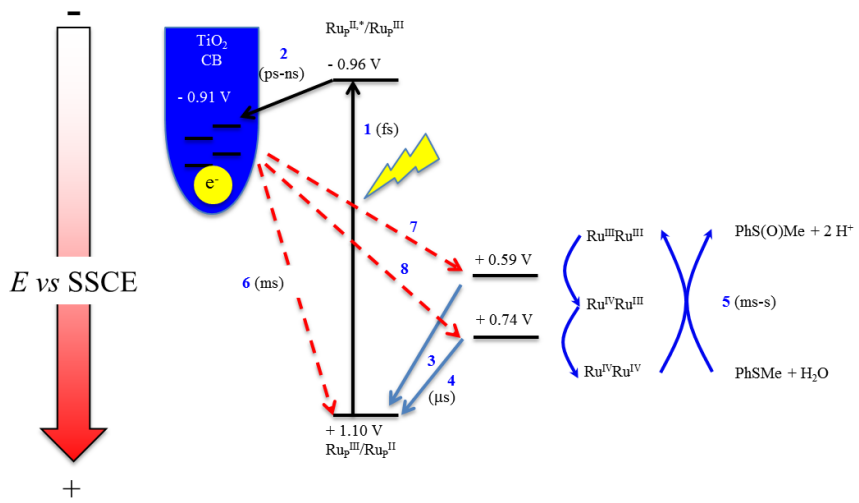

References

[1] T. Faunce, S. Styring, M.R. Wasielewski, G.W. Brudvig, A.W. Rutherford, J. Messinger, A.F. Lee, C.L. Hill, H. deGroot, M. Fontecave, D.R. MacFarlane, B. Hankamer, D.G. Nocera, D.M. Tiede, H. Dau, W. Hillier, L. Wang, R. Amal, Energy Environ. Sci. 6 (2013) 1074.

[2] A. Harriman, Eur. J. Inorg. Chem. (2014) 573.

[3] S. Berardi, S. Drouet, L. Francàs, C. Gimbert-Suriñach, M. Guttentag, C. Richmond, T. Stoll, A. Llobet, Chem. Soc. Rev. (2014), web.

[4] F.P. Rotzinger, S. Munavalli, P. Comte, J.K. Hurst, M. Graetzel, F.J. Pern, A.J. Frank, J. Am. Chem. Soc. 109 (1987) 6619.

[5] P. Comte, M.K. Nazeeruddin, F.P. Rotzinger, A.J. Frank, M. Graetzel, J. Mol. Catal. 52 (1989) 63.

[6] J.L. Cape, J.K. Hurst, J. Am. Chem. Soc. 130 (2008) 827.

[7] L. Duan, Y. Xu, P. Zhang, M. Wang, L. Sun, Inorg. Chem. 49 (2009) 209.

[8] S. Roeser, P. Farràs, F. Bozoglian, M. Martínez-Belmonte, J. Benet-Buchholz, A. Llobet, ChemSusChem 4 (2011) 197.

[9] K. J. Young, L. A. Martini, R. L. Milot, R. C. S. III, V. S. Batista, C. A. Schmuttenmaer, R. H. Crabtree, G. W. Brudvig, Coord. Chem. Rev. 256 (2012) 2503.

[10] Y. Xu, A. Fischer, L. Duan, L. Tong, E. Gabrielsson, B. Åkermark, L. Sun, Angew. Chem., Int. Ed. 49 (2010) 8934.

[11] Y.V. Geletii, Z. Huang, Y. Hou, D.G. Musaev, T. Lian, C.L. Hill, J. Am. Chem. Soc. 131 (2009) 7522.

[12] G. Chen, L. Chen, S.M. Ng, W.L. Man, T.C. Lau, Angew. Chem., Int. Ed. 52 (2013) 1789.

[13] N. Kaveevivitchai, R. Chitta, R. Zong, M. El Ojaimi, R.P. Thummel, J. Am. Chem. Soc. 134 (2012) 10721.

[14] D. L. Ashford, D. J. Stewart, C. R. Glasson, R. A. Binstead, D. P. Harrison, M. R. Norris, J. J. Concepcion, Z. Fang, J. L. Templeton, T. J. Meyer, Inorg. Chem. 51 (2012) 6248.

[15] R.H. Holm, J.P. Donahue, Polyhedron 12 (1993) 571. The data is extracted for Me_2S.

[16] D. Kalita, B. Radaram, B. Brooks, P.P. Kannam, X. Zhao, ChemCatChem 3 (2011) 571.

[17] F. Li, M. Yu, Y. Jiang, F. Huang, Y. Li, B. Zhang, L. Sun, Chem. Commun. 47 (2011) 8949.

[18] S. Ohzu, T. Ishizuka, Y. Hirai, S. Fukuzumi, T. Kojima, Chem. Eur. J. 19 (2013) 1563.

[19] W. Chen, F. Rein, R. Rocha, Angew. Chem., Int. Ed. 121 (2009) 9852.

[20] S. Fukuzumi, T. Kishi, H. Kotani, Y. Lee, W. Nam, Nat. Chem. 3 (2010) 38.

[21] W. Chen, F. Rein, B. Scott, R. Rocha, Chem. Eur. J. 17 (2011) 5595.

[22] M. Hajimohammadi, N. Safari, H. Mofakham, F. Deyhimi, Green Chem. 13 (2011) 991.

[23] O. Hamelin, P. Guillo, F. Loiseau, M. Boissonnet, S. Menage, Inorg. Chem. 50 (2011) 7952.

[24] P. Guillo, O. Hamelin, G. Batat, G. Jonusauskas, N. D. McClenaghan, S. Menage, Inorg. Chem. 51 (2012) 2222.

[25] P. Farras, S. Maji, J. Benet-Buchholz, A. Llobet, Chem. Eur. J. 19 (2013) 7162.

[26] D. Chao, W.F. Fu, Dalton Trans. 43 (2014) 306.

[27] S. Romain, L. Vigara, A. Llobet, Acc. Chem. Res. 42 (2009) 1944.

[28] M.H.V. Huynh, L.M. Witham, J.M. Lasker, M. Wetzler, B. Mort, D.L. Jameson, P.S. White, K.J. Takeuchi, J. Am. Chem. Soc. 125 (2003) 308.

[29] C. Di Giovanni, A. Poater, J. Benet-Buchholz, L. Cavallo, M. Solà, A. Llobet, Chem. Eur. J. 20 (2014) 3898.

[30] W. Singh, D. Pegram, H. Duan, D. Kalita, P. Simone, G. Emmert, X. Zhao, Angew. Chem., Int. Ed. 51 (2011) 1653.

[31] W. Youngblood, S. Lee, Y. Kobayashi, E. Hernandez-Pagan, P. Hoertz, T. Moore, A. Moore, D. Gust, T. Mallouk, J. Am. Chem. Soc. 131 (2009) 926.

[32] R. Brimblecombe, A. Koo, G. Dismukes, G. Swiegers, L. Spiccia, J. Am. Chem. Soc. 132 (2010) 2892.

[33] L. Li, L. Duan, Y. Xu, M. Gorlov, A. Hagfeldt, L. Sun, Chem. Commun. 46 (2010) 7307.

[34] W. Song, C. R. K. Glasson, H. Luo, K. Hanson, M. K. Brennaman, J. J. Concepcion, T. J. Meyer, J. Phys. Chem. Lett. 2 (2011) 1808.

[35] G.F. Moore, J.D. Blakemore, R.L. Milot, J.F. Hull, H.E. Song, L. Cai, C.A. Schmuttenmaer, R.H. Crabtree, G.W. Brudvig, Energy Environ. Sci. 4 (2011) 2389.

[36] Y. Gao, X. Ding, J. Liu, L. Wang, Z. Lu, L. Li, L. Sun, J. Am. Chem. Soc. 135 (2013) 4219.

[37] L. Alibabaei, M.K. Brennaman, M.R. Norris, B. Kalanyan, W. Song, M.D. Losego, J.J. Concepcion, R.A. Binstead, G.N. Parsons, T.J. Meyer, Proc. Natl. Acad. Sci. USA 110 (2013) 20008.

[38] Y. Gao, L. Zhang, X. Ding, L. Sun, Phys. Chem. Chem. Phys. 16 (2014) 12008.

[39] X. Ding, Y. Gao, L. Zhang, Z. Yu, J. Liu, L. Sun, ACS Catal. 4 (2014) 2347.

[40] J.R. Swierk, T.E. Mallouk, Chem. Soc. Rev. 42 (2013) 2357.

[41] M.K. Brennaman, A. Patrocinio, W. Song, J. Jurss, J.J. Concepcion, P. Hoertz, M. Traub, N. Murakami Iha, T.J. Meyer, ChemSusChem 4 (2011) 216.

[42] W. Song, M.K. Brennaman, J.J. Concepcion, J. Jurss, P. Hoertz, H. Luo, C. Chen, K. Hanson, T.J. Meyer, J. Phys. Chem. C 115 (2011) 7081.

[43] W. Song, A.K. Vannucci, B.H. Farnum, A.M. Lapides, M.K. Brennaman, B. Kalanyan, L. Alibabaei, J.J. Concepcion, M.D. Losego, G.N. Parsons, T.J. Meyer, J. Am. Chem. Soc. 136 (2014) 9773.

[44] M. Antoniadou, P. Lianos, Catal. Today 144 (2009) 166.

[45] M. Antoniadou, D.I. Kondarides, D. Labou, S. Neophytides, P. Lianos, Solar Energ. Mat. Sol. C. 94 (2010) 592.

[46] P. Péchy, F.P. Rotzinger, M.K. Nazeeruddin, O. Kohle, S.M. Zakeeruddin, R. Humphry-Baker, M. Grätzel, J. Chem. Soc., Chem. Commun. (1995) 65.

[47] K. Hanson, M.K. Brennaman, H. Luo, C.R.K. Glasson, J.J. Concepcion, W. Song, T.J. Meyer, ACS Appl. Mater. Interfaces 4 (2012) 1462.

[48] F. Lakadamyali, A. Reynal, M. Kato, J.R. Durrant, E. Reisner, Chem. Eur. J. 18 (2012) 15464.

[49] J.N. Clifford, E. Palomares, M.K. Nazeeruddin, M. Grätzel, J.R. Durrant, J. Phys. Chem. C 111 (2007) 6561.

[50] I. Montanari, J. Nelson, J.R. Durrant, J. Phys. Chem. B 106 (2002) 12203.

[51] A. Fujishima, K. Honda, Nature 238 (1972) 37.